General Properties of Power Losses in Soft Ferromagnetic Materials

GIORGIO BERTOTTI

Abstract—**Measurements are reported of the loss per cycle (sinusoidal flux waveform) versus magnetizing frequency f_m ($0 \le f_m \le 100$ or 400 Hz) and peak magnetization I_{max}, performed on three-percent SiFe alloys (both grain oriented and nonoriented), Armco iron, NiFe alloys, and amorphous ribbons. By making use of a new theoretical framework, we discuss the microscopic origin of the observed dynamic losses, and we give a physical interpretation of the general fact that the loss per cycle is always a nonlinear function of f_m. In particular, we show that the dynamic loss per cycle approximately follows, for a wide variety of different materials, a simple law of the form $k_1 f_m + k_2 \sqrt{f_m}$, where the first term represents the classical contribution. In the case of microcrystalline nonoriented laminations, the theory permits one to calculate the absolute value of the constant k_2 directly in terms of the values of the hysteresis loss and the average grain size, obtaining good agreement with experiments. Finally, a theoretical procedure is discussed by which it is possible, for a generic material, given a single loss curve at a certain value of I_{max}, to predict the dependence of dynamic losses on both I_{max} and f_m, with an approximation within ± 10 percent in all the investigated cases. The behavior of grain-oriented SiFe, which presents some specific complexities, is discussed in particular detail.**

I. Introduction

THE AIM of the present paper is to provide a contribution to the understanding of magnetic losses in soft metallic ferromagnetic materials that may be useful both to the fundamental physicist interested in microscopic magnetization processes and to the engineer involved in the electrotechnical applications of soft steels. Basically, we shall examine the dependence of power losses on magnetizing frequency f_m and peak magnetization I_{max}, trying to clarify how this dependence is related to the parameters like grain size that define the microstructure of a given material, as well as to those like domain size that characterize its magnetic domain structure. Our starting point will be a simple and important phenomenological principle, which has been commonly adopted in loss investigations for a long time, the so-called separation of losses [1], [2]. According to it, the average power loss per unit volume P of any material is decomposed into the sum of a hysteresis and a dynamic contribution, which are separately investigated,

$$P = P^{(\mathrm{hyst})} + P^{(\mathrm{dyn})} \tag{1}$$

Manuscript received December 10, 1986; revised May 23, 1987. This work was supported in part by the Italian Ministry of Education and the Progetto Finalizzato Energetica, under Grant CNR-ENEA.

The author is with the Istituto Elettrotecnico Nazionale Galileo Ferraris and GNSM-CISM, I-10125 Torino, Italy.

IEEE Log Number 8717384.

with $P^{(\mathrm{hyst})}$ equal to the area of the quasi-static hysteresis loop times f_m. The physical reason for such a decomposition is that $P^{(\mathrm{hyst})}$ originates from the discontinuous character of the magnetization process at a very microscopic scale, whereas $P^{(\mathrm{dyn})}$ is associated with the macroscopic large-scale behavior of the magnetic domain structure. In fact, a proper statistical treatment of the loss problem [3], [4] shows that (1) is naturally obtained whenever the characteristic time scales of these two processes do not overlap.

The important conceptual simplification introduced by the separation of losses is readily appreciated, because the interpretation of $P^{(\mathrm{dyn})}$—the quantity of principal interest in this paper—can then be based on simple macroscopic domain models, paying no heed to the intricate fine-scale details of wall motion. In this connection, the so-called "classical" model [2], [5] even disregards the very presence of magnetic domains and assumes a magnetization process perfectly homogeneous in space. In the case of a lamination of thickness d and in the range of magnetizing frequencies where the skin effect is negligible, this model predicts (sinusoidal flux waveform)

$$P^{(\mathrm{dyn})} \equiv P^{(\mathrm{class})} = \pi^2 \sigma d^2 I_{max}^2 f_m^2 / 6 \tag{2}$$

where σ is the electrical conductivity of the material. The classical model is, however, too gross a simplification. As a consequence of domain effects, the dynamic loss $P^{(\mathrm{dyn})}$ is generally found to be definitely larger than $P^{(\mathrm{class})}$, the difference between them, called excess loss $P^{(\mathrm{exc})}$, being in many cases larger than $P^{(\mathrm{class})}$ itself. By expressing the total loss as

$$P = P^{(\mathrm{hyst})} + P^{(\mathrm{class})} + P^{(\mathrm{exc})}, \tag{3}$$

the central problem becomes then to understand the origin and the properties of the excess term $P^{(\mathrm{exc})}$.

The guideline in the interpretation of excess losses has been, for a long time, the model proposed by Pry and Bean [6], in which the dynamic loss of an infinite lamination containing a periodic array of longitudinal domains of width $2L$ is calculated from Maxwell's equations. This model indicates that the fundamental parameter controlling excess losses should be the ratio $2L/d$ between the domain size and the lamination thickness and predicts

$$P^{(\mathrm{exc})} \ll P^{(class)}, \quad \text{when } 2L/d \ll 1$$

$$P^{(\mathrm{exc})} \simeq \left(1.63\,\frac{2L}{d} - 1\right) P^{(\mathrm{class})}, \quad \text{when } 2L/d \gg 1. \tag{4}$$

In spite of its remarkable achievements, however, even the Pry and Bean model turns out to be of limited validity, essentially because of its highly idealized character. In microcrystalline materials, in fact, it is commonly found that $P^{(\mathrm{exc})} \sim P^{(\mathrm{class})}$ even if $2L/d \ll 1$ [7]–[9]. On the other hand, $P^{(\mathrm{exc})}/f_m$ shows in general a nonlinear dependence on f_m, which cannot be easily explained in terms of (4) [7]. In the case of single crystals or grain-oriented laminations having $2L/d \gg 1$, the departure of measured losses from Pry and Bean predictions has been related to various effects, like the presence of irregularities in the wall motion, domain multiplication, or wall bowing [10]–[16]. As to fine-grained materials, attempts have been made to connect excess losses with Barkhausen noise [17], or to attribute them to continuous rearrangements of the domain configuration [18]. However, no general agreement as to the role of all these mechanisms in determining the actual loss features of soft materials has yet been achieved.

A new conceptual framework, capable of including most of these effects in a unified treatment has been proposed recently by the author, on the basis of a statistical approach to the loss phenomenology. The theory, developed in [3], [4], [19]–[22] and here briefly reviewed in Section II, leads to the conclusion that the large-scale behavior of magnetic domains can be described in terms of the dynamics of $\tilde{n}$ statistically independent magnetic objects (MO), each corresponding to a group of neighboring interacting domain walls, and reduces the loss problem to the investigation of the main physical properties of $\tilde{n}$ as a function of f_m, $I_{\max}$, and the material microstructure. This approach can be successfully applied to a variety of different materials, by investigating the physical meaning of the concept of MO in each case. In particular, it has been shown that a single MO can be identified with a single Bloch wall in grain-oriented materials with large domains [20], whereas, in microcrystalline materials, the whole domain structure inside a single grain plays the role of a single MO [21], [22].

Starting from these premises, in this paper we present the results of a twofold investigation. In the first place, we have carried out a systematic experimental study of the loss behavior versus $I_{\max}$ and f_m in various soft magnetic materials, consisting of measurements of the loss per cycle versus f_m (in the range $0 \leq f_m \leq 100$ or 400 Hz, depending on the material) performed—at several values of peak magnetization $I_{\max}$—on SiFe alloys of different texture and grain size, Armco iron, NiFe alloys, and amorphous ribbons. By these results, reported in Section III, we have tried to provide a source of information on the properties of eddy current losses in soft materials, as well as a basis for a proper testing of theoretical loss models. In this connection, our second goal has been to interpret these experimental results in terms of the mentioned dynamics of MO's, and to relate the observed properties of the parameter $\tilde{n}$ to the microstructure and the domain structure of the investigated materials. As fully discussed in Sections III and IV, several interesting conclusions have been obtained by this analysis. First, the theory gives a natural interpretation of the general fact that the dynamic loss per cycle is a nonlinear function of f_m, and shows, in particular, that this nonlinearity is approximately consistent with a simple law $P^{(\mathrm{exc})}/f_m \simeq k_2\sqrt{f_m}$ for a wide variety of materials. Secondly, the theory is also applicable to nonoriented, microcrystalline laminations having a fine domain structure ($2L/d \ll 1$). In this case, the absolute value of the constant k_2 can be calculated, under reasonable assumptions, directly in terms of the values of the hysteresis loss and the average grain size, obtaining good agreement with experimental results. Finally, the theory reduces the dependence of excess losses on both $I_{\max}$ and f_m to a common mechanism, the competition between the applied field and highly inhomogeneous internal counterfields governing the dynamics of the single MO's. This feature of the theory has important practical consequences, since it permits one to extract the dependence of dynamic losses on both $I_{\max}$ and f_m from a single loss curve at a given value of $I_{\max}$ and to express this dependence in closed analytic form. In particular, it will be shown in Section IV that, in the case of grain-oriented three-percent SiFe, the knowledge of only two points of a single loss curve permits one to predict the loss behavior versus $I_{\max}$ and f_m with an approximation that, for the data presented in this paper and in the range $f_m \gtrsim 20$ Hz, is within ± 10 percent.

II. Statistical Interpretation of Eddy Current Losses

According to the statistical theory of eddy current losses developed in [3], [4], [19]–[22], the basic physical mechanism governing excess losses in soft materials is identified with the competition between the external magnetic field, applied uniformly in the sample, and highly inhomogeneous local counterfields due to eddy currents and microstructural interactions. The basic consequences of this physical interpretation are fully discussed in the references mentioned and can be summarized as follows.

1) For each value of the average magnetization rate $\dot{I} = 4I_{\max}f_m$, the magnetization process in a given cross section of the magnetic lamination can be described, as anticipated in the introduction, in terms of $\tilde{n}$ simultaneously active magnetic objects. The dynamic behavior of a single MO is controlled by an equation of the form $H_{\mathrm{exc}} \propto \dot{\Phi}$, where $H_{\mathrm{exc}} = P^{(\mathrm{exc})}/\dot{I}$ is the excess dynamic field acting on the MO, $\dot{\Phi}$ is the magnetic flux rate of change correspondingly provided by the MO, and the proportionality constant is determined by the damping effect of eddy currents [20], [23]. When there are $\tilde{n}$ simultaneously active MO's, $\dot{\Phi}$ must be, on the average, a fraction $1/\tilde{n}$ of the total flux rate $S\dot{I}$ imposed to the sample (S is the cross-sectional area of the lamination), so that a

relationship of the form $H_{exc} \propto 1/\tilde{n}$ is expected, which actually turns out to be [20]

$$H_{exc} \equiv P^{(exc)}/\dot{I} = H^{(w)}/\tilde{n} \tag{5}$$

where

$$H^{(w)} = \sigma G^{(w)} S\dot{I} = 4\sigma G^{(w)} S I_{max} f_m \tag{6}$$

and the value of the dimensionless coefficient $G^{(w)}$ is $G^{(w)} = (4/\pi^3)[\Sigma_k 1/(2k+1)^3] = 0.1356$.

2) The fundamental property of the quantity $\tilde{n}$ appearing in (5) is that it is expected to be a function $\tilde{n}(H_{exc}; \{P\})$ of the excess field H_{exc} and of some set $\{P\}$ of parameters characterizing the microstructure and domain structure of different materials, monotonically increasing with increasing H_{exc} [20]. Notice that, if this function is known, we obtain, from (5),

$$H_{exc}\tilde{n}(H_{exc}; \{P\}) = H^{(w)} \tag{7}$$

which can be solved with respect to H_{exc}, thus determining the dependence of the excess loss $P^{(exc)} = \dot{I}H_{exc}$ on $H^{(w)}$ (i.e., on I_{max} and f_m, see (6)) and on $\{P\}$. However, since $\tilde{n}(H_{exc}; \{P\})$ is an increasing function of H_{exc}, the dependence of H_{exc} on $H^{(w)}$ will be in general less than linear, and a definite curvature in the excess loss per cycle will be obtained. The theory gives, therefore, a natural interpretation of the fact, already known in the literature and confirmed by the experiments reported in this paper, that the loss per cycle is ordinarily a nonlinear function of magnetizing frequency.

3) Several iron-based alloys obey the simple linear law

$$\tilde{n}(H_{exc}; \{P\}) = \tilde{n}_0 + H_{exc}/V_0 \tag{8}$$

where the microstructural information is now carried by $\tilde{n}_0$, which represents the limiting number of simultaneously active MO's when $f_m \to 0$, and by the magnetic field V_0. Equations (7) and (8) lead to the nonlinear excess loss expression

$$\begin{aligned} H_{exc} &\equiv P^{(exc)}/\dot{I} \\ &= \tilde{n}_0 V_0 \left(\sqrt{1 + 4\sigma G^{(w)} S\dot{I}/\tilde{n}_0^2 V_0} - 1\right)/2 \\ \dot{I} &= 4 I_{max} f_m. \end{aligned} \tag{9}$$

In the following sections, we shall undertake a general study of the properties of the function $\tilde{n}(H_{exc}; \{P\})$ in different materials to clarify the real value and applicability of the proposed theoretical approach to magnetic losses, and, in particular, the physical meaning and range of validity of the linear law (8). Before passing to the presentation of the experimental results, however, we want to recall a simple and useful procedure, already proposed in [20], by which the function $\tilde{n}(H_{exc}; \{P\})$ can be directly obtained from experiments. According to (5), $\tilde{n} = H^{(w)}/H_{exc}$ is determined by the values of $H^{(w)}$ and H_{exc}. Both of these quantities can be directly evaluated from experiments, as can be seen from their very definition. Therefore, if we plot a generic loss curve in terms of $H^{(w)}/H_{exc}$ versus H_{exc}—instead of P/f_m versus f_m as usual—we shall directly obtain the behavior of the function $\tilde{n}(H_{exc}; \{P\})$. It is interesting to notice that a quite similar loss representation has also been proposed and used, although on more empirical bases, in [14], [15]. According to the physical interpretation summarized in 2), $\tilde{n}$ is expected to depend explicitly on H_{exc} only, while other quantities (e.g., I_{max}) should have only an indirect influence, through induced changes of the parameters $\{P\}$. This means that we may obtain valuable information on the microstructural properties of different materials, or on the modifications of the domain structure behavior upon changing I_{max} in a same material, simply by using the $\tilde{n}$ versus H_{exc} representation. For example, if no changes occur in the magnetic domain structure of a given material as a function of I_{max}, we expect that the loss curves referring to different values of I_{max} should all reduce to a single curve, when represented in terms of $\tilde{n}$ versus H_{exc}. This is the point of view that will be adopted in the discussion of the experimental results reported in the following section.

III. Experimental Results and Discussion

Losses were measured on grain oriented (GO) and nonoriented (NO) three-percent SiFe alloys, Armco iron, mumetal, 50–50 NiFe alloys, and amorphous materials, as listed in Table I. Two sample geometries were employed in the experiments: standard Epstein frames and toroidally wound ribbons. The power loss was obtained by means of a high precision analogic wattmeter, permitting measurements at controlled sinusoidal magnetic flux waveform in the range of magnetizing frequencies 1–400 Hz. The hysteresis loss was measured in general through the ballistic method. In the case of NO SiFe and Armco iron, however, where the error in the ballistic evaluation of the hysteresis loss was found to be comparable with the variations of dynamic loss at low f_m, the hysteresis loss was obtained by directly extrapolating the dynamic loss curve down to $f_m \to 0$. For each sample, the loss behavior in the range $0 \le f_m \le 100$ Hz ($0 \le f_m \le 400$ Hz for the amorphous ribbons), and at several (four to five) values of peak magnetization I_{max} was determined.

The obtained P/f_m versus f_m curves are reported in Figs. 1–10 (left-hand portion of each figure). In the right-hand part of the figures, the very same results are reported in terms of $\tilde{n}(H_{exc}; \{P\})$ versus H_{exc}, according to the representation discussed in Section II. We shall now examine these results in more detail, focusing our attention, in the first place, on GO and NO SiFe, because these two cases exhibit some basic features of power losses common, to some extent, to all the investigated materials.

Grain Oriented Three-Percent SiFe

Fig. 1(a) reports the behavior of the loss per cycle and unit mass $P/\delta f_m$ (δ is the density of the material) versus f_m, measured at five different values of I_{max}. The corresponding representation in the plane (H_{exc}, $\tilde{n}$) is given in Fig. 1(b). This representation clearly shows the fact, already stressed in previous works [20], that GO SiFe is a

TABLE I

Figure Number	Material Properties	Density (10^3 Kg/m^3)	Conductivity (10^6 Ω^{-1}m^{-1})	Grain Size (10^{-4} m)	Sample Geometry	Thickness (10^{-4} m)	Cross Section Area (10^{-6} m^2)	50 Hz Losses (W/kg) I_{max} (Tesla)	$P^{(hyst)}$	$P^{(class)}$	$P^{(exc)}$ Experimental	$P^{(exc)}$ Calculation from (17)
1,2	grain-oriented 3% SiFe longitudinally cut	7.65	2.2		Epstein frames	2.9	8.7	1.7	0.34	0.29	0.53	
10	grain-oriented 3% SiFe transversally cut (90°)	7.65	2.2			3.4	10.2	1.5	1.7	0.31	1.8	
3	nonoriented 3% SiFe	7.65	2	0.85		3.5	10.5	1.5	1.8	0.29	0.33	0.31
4	nonoriented 3% SiFe	7.65	2	1		3.4	10.2	1.5	2.1	0.28	0.41	0.39
5	Armco iron	7.86	9.3	0.38		1.2	3.6	1.5	3.6	0.16	0.48	0.43
6	Mumetal	8.6	2	0.48	wound	1.5	4.5	0.65	0.021	$9.3\ 10^{-3}$	0.012	0.007
9	50-50 NiFe	8.25	2.2		ribbons	1	2	1.5	0.51	0.02	0.31	
7	amorphous METGLAS 2605 SC	7.3	0.8			0.5	0.25	1.5	0.2	$2.5\ 10^{-3}$	0.08	
8	amorphous METGLAS 2605 CO	7.56	0.77			0.3	0.15	1.5	0.29	$8.5\ 10^{-4}$	0.094	

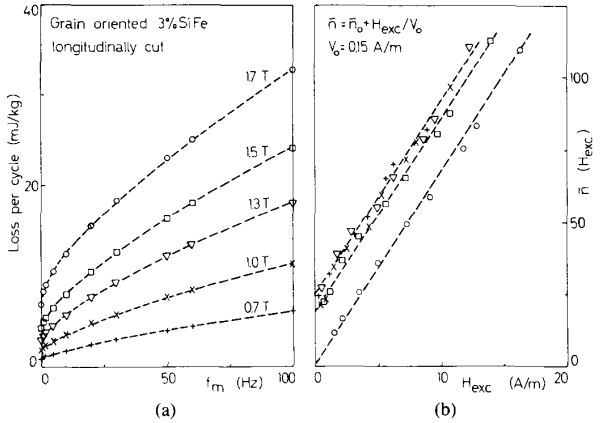

(a) (b)

Fig. 1. (a) Loss per cycle and unit mass (sinusoidal flux waveform) versus magnetizing frequency in grain oriented three-percent SiFe, at different values of peak magnetization I_{max} (see Table I for further information). Various symbols represent experimental loss points (their size is larger than uncertainty of measured values), broken lines are theoretical curves calculated from (2), (3), (9), with values of parameters $\tilde{n}_0$ and V_0 obtained as discussed below. (b) Representation of same experimental points in terms of parameter $\tilde{n}$, defined by (5) and (6), versus dynamic field $H_{exc} = P^{(exc)}/4I_{max}f_m$. It can be seen that, in this representation, single loss curves become definite straight lines of form (8). Their slope determines field V_0, while $\tilde{n}_0$ is given by their intersection with $\tilde{n}$ axis. Numerical values of $\tilde{n}_0$ and V_0 are easily obtained by least square method. It is found that V_0 has always constant value $V_0 = 0.15$ A/m, independent of I_{max}, while $\tilde{n}_0 = 1$ when $I_{max} = 1.7$ T, $\tilde{n}_0 = 19$ when $I_{max} = 1.5$ T and $\tilde{n}_0 = 25$ when $I_{max} \leq 1.3$ T.

case where the linear law (8) for the dependence of $\tilde{n}$ on H_{exc} is strictly followed. We point out that this result cannot be merely interpreted in terms of a first-order expansion of $\tilde{n}(H_{exc}; \{P\})$ around $H_{exc} = 0$, since the linear term H_{exc}/V_0 is by no means small with respect to $\tilde{n}_0$, as can be easily checked directly from Fig. 1(b). The values of the parameters $\tilde{n}_0$ and V_0 associated with the different loss curves are easily obtained by a least-square linear fitting of the experimental points in the $(H_{exc}, \tilde{n})$ plane, shown by the broken straight lines in Fig. 1(b). We obtain $V_0 = 0.15$ A/m, independent of I_{max}, whereas $\tilde{n}_0$ increases from $\tilde{n}_0 \simeq 1$, when $I_{max} = 1.7$ T, up to $\tilde{n}_0 \simeq 25$ when $I_{max} \lesssim 1$ T. The knowledge of $\tilde{n}_0$ and V_0 permits one to predict, through (2), (3), (9), the behavior of $P/\delta f_m$ versus f_m and I_{max}. The broken lines in Fig. 1(a) have been obtained just by this procedure. One can notice the excellent agreement with experimental points, and, in particular, the ability of (9) to describe the observed loss nonlinearities. This result leads to a first, interesting conclusion about the behavior of excess losses in GO SiFe. Equation (9) implies in fact, that, for sufficiently high values of f_m (commonly above a few Hz) the excess loss per cycle can be approximated as

$$P^{(exc)}/f_m \simeq 8I_{max}\left(\sqrt{\sigma G^{(w)} S V_0 I_{max} f_m} - \tilde{n}_0 V_0/4\right) \quad (10)$$

and therefore becomes essentially proportional to $\sqrt{f_m}$. Thus the statement, often found in the literature [2], [24], that dynamic loss nonlinearities are limited to low magnetizing frequencies, seems somewhat inaccurate. Our results show, on the contrary, that such nonlinearities approximately obey a simple $\sqrt{f_m}$ law in the whole investigated f_m range, so that the dependence of the total loss per cycle P/f_m on f_m is essentially of the form

$$P/f_m \simeq k_0 + k_1 f_m + k_2\sqrt{f_m} \quad (11)$$

where the meaning of k_0, k_1, k_2 can be easily deduced from (2), (3), (10). It can be checked from (8), that, in the f_m range where $P^{(exc)}/f_m \propto \sqrt{f_m}$, the number $\tilde{n}$ of active MO's increases essentially as $\sqrt{f_m}$. This conclusion is in good agreement with the results reported in [14], [15], [25].

The fact that the field V_0 is found to be independent of I_{max} makes it an intrinsic parameter of the material, connected to its microstructural properties, rather than a simple fitting parameter. We shall see that this interesting conclusion applies to most of the materials following the linear law (8). It has been suggested in a previous paper [20] that the microstructural interpretation of V_0 should involve a relation of the form $V_0 \sim H_{hyst}/N_0$ between V_0, the quasi-static coercive field H_{hyst}, and the number N_0 of MO's available for magnetization in a given cross section of the material. While the meaning and validity of this connection in GO SiFe needs further study and will be analyzed in a future paper, a possible interpretation of its origin in microcrystalline materials like NO SiFe has been recently proposed [21], [22] and will be discussed in the next subsection.

As to the dependence of $\tilde{n}_0$ on I_{max}, we recall that $\tilde{n}_0$ represents, according to (8), the number of MO's which are simultaneously active in the limit of low magnetizing frequencies, and that, in the material under consideration, each MO essentially coincides with a single Bloch wall. As previously pointed out, $\tilde{n}_0 \simeq 25$ at low I_{max}, a value which is of the order of the number of walls present in the cross section of the investigated sample in the demagnetized state. This indicates that a fairly regular and coherent motion of all walls takes place at low I_{max}. The progressive onset of irregularities in the wall motion with increasing I_{max} is then clearly pointed out by the steady decrease of $\tilde{n}_0$, down to $\tilde{n}_0 \sim 1$ (one active MO at a time), which represents a quite general lower limit for the values of $\tilde{n}_0$ in any material [20]. An interesting test of the physical meaning of $\tilde{n}_0$ can be made by considering the modifications in the loss behavior consequent to different procedures of sample demagnetization. Each of the loss curves reported in Fig. 1(a) refers to a sample preliminarily demagnetized at a frequency of 1 Hz. If the same measurements are performed after 50 Hz demagnetization, different results are obtained. The example reported in Fig. 2(a) refers to $I_{max} = 0.7$ T and shows a definite dynamic loss decrease after 50 Hz demagnetization. This effect progressively disappears when higher values of I_{max} are considered. These results can be explained qualitatively by noticing that, by demagnetizing the sample at 50 Hz, we activate domain multiplication processes that introduce a higher number of domain walls in the sample cross section, with a consequent reduction of the excess loss. The newly generated walls, however, are easily annihilated at high inductions, and this explains why the loss behavior is affected by demagnetization only when $I_{max} \lesssim 1$ T. However, this interpretation does become really evident and expressible in quantitative terms when the same loss data are represented in the plane $(H_{exc}, \tilde{n})$ (Fig. 2(b)). The difference between the two loss curves results now in an increase of $\tilde{n}_0$, from $\tilde{n}_0 \simeq 25$ up to $\tilde{n}_0 \simeq 40$, indicating the higher number of domain walls introduced in the sample cross section, while the slope $1/V_0$ of the loss lines has not changed at all, as expected from the mentioned microstructural character of the field V_0.

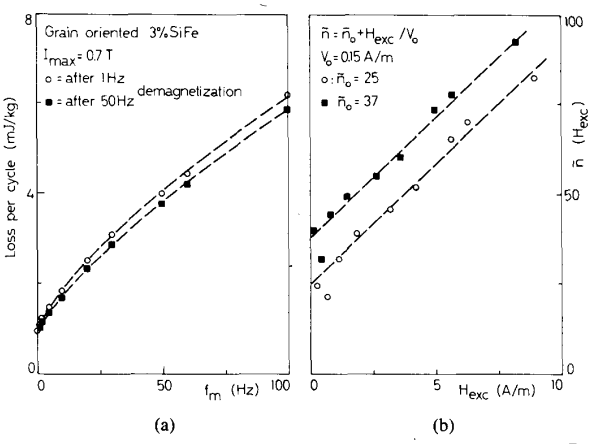

Fig. 2. Modifications in loss behavior of grain oriented three-percent SiFe at $I_{max} = 0.7$ T, consequent to different procedures of sample demagnetization. See caption of Fig. 1 for meaning of employed representation.

As a final remark, we point out that the linear law (8) is strictly followed by GO SiFe even after extensive plastic straining or upon the application of external tensile stresses [20] and well describes also the behavior of three-percent SiFe (110) [001] single crystals [19], [20].

Nonoriented Three-Percent SiFe and Other Materials Following the Linear Law $\tilde{n} = \tilde{n}_0 + H_{exc}/V_0$

Figs. 3 and 4 report the loss behavior measured on two laminations of NO three-percent SiFe, characterized by different grain size and coercivity. In these materials, the average size of magnetic domains is certainly smaller than the grain size, which, in turn, is smaller than the lamination thickness (see Table I). As discussed in the Introduction, any model similar to that of Pry and Bean would predict, in this case, no excess loss at all (see (4)), in clear contradiction with the experimental data reported in Figs. 3(a) and 4(a). We will show now how this contradiction can be resolved by making use of the theory discussed in Section II.

A first result of interest is that, as shown by Figs. 3(b) and 4(b), the linear law (8) is still fulfilled. However, contrary to the case of GO SiFe, the term H_{exc}/V_0 is now predominant at all values of I_{max} and f_m of interest. The parameter $\tilde{n}_0$ does not play any significant role and can be neglected. Physically, this simply means that the number of new MO's becoming active in dynamic conditions soon destroys any memory of the quasi-static state described by $\tilde{n}_0$. Equations (8) and (9) can then be conveniently approximated as

$$\tilde{n}\left(H_{exc}; \{P\}\right) = H_{exc}/V_0 \tag{12}$$

$$P^{(exc)} = \dot{I}\sqrt{H^{(w)}V_0} = 8\sqrt{\sigma G^{(w)} S V_0}\,(I_{max} f_m)^{3/2}. \tag{13}$$

Equations (12) and (13) have a number of remarkable consequences. Assuming, in analogy with the results obtained in GO SiFe, that V_0 is an intrinsic parameter of the material, independent of I_{max}, we expect from (12) that all

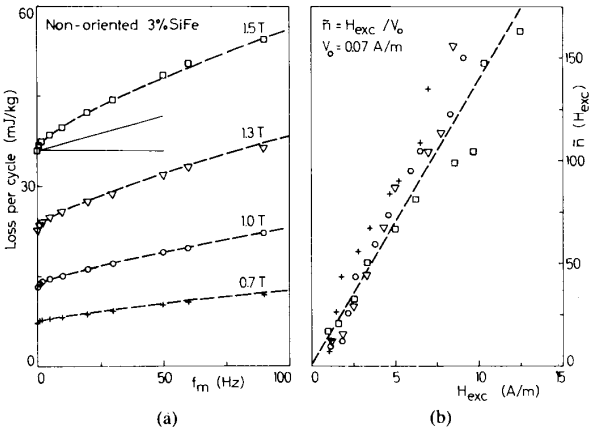

Fig. 3. Power losses in nonoriented three-percent SiFe. Comment to figure is analogous to that of Fig. 1. For this material, (8) can be approximated by (12), which does not contain parameter $\tilde{n}_0$. Value of field V_0 determined from (H_{exc}, $\tilde{n}$) representation of experimental points is $V_0 = 0.07$ A/m. Two continuous straight segments in Fig. 3(a) represent hysteresis and classical contributions.

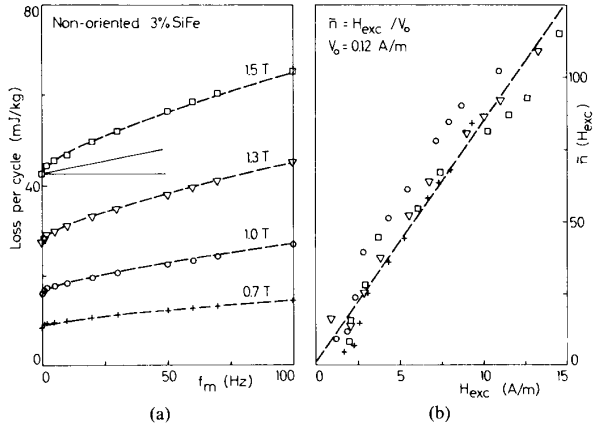

Fig. 4. Same as in Fig. 3, for sample where $V_0 = 0.12$ A/m.

loss points at different values of I_{max} should reduce to a single straight line, when represented in the plane (H_{exc}, $\tilde{n}$). This prediction is well confirmed, apart from some scattering of the data related to the precision of the measurements, by Figs. 3(b) and 4(b). In terms of the behavior of P/f_m versus f_m, this implies that the single parameter V_0 determines, through (2), (3), (13), the complete dependence of dynamic losses on I_{max} and f_m, and, in particular, that the excess loss per cycle follows a simple $\sqrt{f_m}$ law. The broken lines in Figs. 3(a) and 4(a) were calculated from (2), (3), and (13), assuming in each case the fixed value of V_0 obtained from the corresponding (H_{exc}, $\tilde{n}$) representation: $V_0 = 0.07$ A/m in Fig. 3(a) and $V_0 = 0.12$ A/m in Fig. 4(a).

It is evident that the fundamental problem at this point is to justify, on physical grounds, the absolute value of the field V_0, so as to explain the microstructural reason for the presence of an excess loss contribution in magnetic laminations having domains definitely smaller than their thickness. A possible key to this problem has been proposed recently in [21], [22], on the basis of the following schematic description of the magnetization process in fine-grained materials. Adopting a point of view slightly different from that of Section II, we can equivalently interpret a single MO as a region of the material cross section characterized by a fairly homogeneous local coercive field, so that it will become active as a whole when the applied field overcomes a given threshold. In an annealed, fine grained lamination, where the main fluctuations of local coercive field are expected to take place from grain to grain, a single MO is then naturally identified with the whole domain structure delimited by the cross section of a single grain, so that the total number of MO's present in a given cross section of area S of the lamination will be

$$N_0 = S/s^2 \tag{14}$$

with s equal to the average grain size. The statistical distribution of the values of local coercive field at which different MO's will become active can be assumed to be, to a first approximation, flat, with constant density $1/V_0$ (the field V_0 represents therefore the average minimum separation between different local coercive field values). As fully discussed in [22], these assumptions imply that in dynamic conditions, when the applied field is greater than its corresponding quasi-static value by the amount H_{exc}, all the MO's inside a portion of width H_{exc} of the mentioned distribution of local coercive fields will be simultaneously active. Since this number is simply $\tilde{n} = H_{exc}/V_0$, (8) is straightforwardly obtained. On the other hand, as a consequence of its very definition, the field V_0 must be directly related to the macroscopic quasi-static coercive field H_{hyst} of the material. In fact, as shown in [21], [22], the value of H_{hyst} in the loop of peak magnetization I_{max} is related to V_0 by the expression

$$H_{hyst} = N_0 V_0 I_{max}/2\langle I_s \rangle \tag{15}$$

where N_0 is given by (14) and $\langle I_s \rangle$ is the value of macroscopic magnetization when all grains are saturated, each along its most favored easy magnetization axis ($\langle I_s \rangle \simeq 0.85 I_s$ in a material of positive cubic anisotropy having a perfectly isotropic distribution of crystallographic grain orientations). From (14), (15), (13), we obtain

$$V_0 = 2s^2 H_{hyst} \langle I_s \rangle / S I_{max} \tag{16}$$

$$P^{(exc)} = 8 I_{max} f_m \sqrt{2\sigma G^{(w)} s^2 \langle I_s \rangle H_{hyst} f_m} \tag{17}$$

where, in the comparison of the model with experiments, the most convenient definition of H_{hyst}, not related to any specific assumption about the shape of the magnetization loop, is $H_{hyst} = P^{(hyst)}/4 I_{max} f_m$. Equation (17) predicts that the excess loss per cycle of the fine-grained materials should be proportional to $\sqrt{f_m}$ and expresses the loss absolute value at a given magnetizing frequency directly in terms of the hysteresis loss and the average grain size, without any adjustable parameter. As shown by the data reported in Table I, the predictions of (17) are in good

agreement with the excess losses observed in the two NO SiFe laminations considered in Figs. 3 and 4. The validity and range of applicability of (17) have been tested more extensively in [9], [21], [22], where it is shown that (17) is actually capable of reproducing, to a good approximation, a number of loss results in NO three-percent SiFe laminations spanning a much wider range of grain size values (from $\sim 30\ \mu$m to $\sim 300\ \mu$m). It is worth remarking, however, that the whole picture presented here is expected to fail when the grain size becomes larger than the sample thickness. Actually, in these conditions, the inhomogeneities of local coercive field inside each grain become more and more important. Each grain splits into several independent MO's and, with further increasing grain size, the material progressively approaches the condition where the single Bloch walls, rather than the single grains, act as individual MO's.

It is natural to ask now if other materials, besides NO SiFe, do behave according to (17). Figs. 5 and 6 report the results of loss measurements on Armco iron and Mumetal. The uncertainty in the loss absolute values is rather large in the case of Mumetal, due to the very low loss of this material. Anyway, it can be seen from these figures and the data reported in Table I that the considerations made for NO SiFe remain essentially valid. Fig. 7 reports a final case where the linear law (8) is obeyed, that of a wound ribbon of the amorphous alloy Metglas 2605 SC. Although the microstructural properties of this material are completely different from those of GO SiFe, and the domain structure is extremely intricate, we find a rather similar behavior of the function $\tilde{n}(H_{exc}; \{P\})$. The field V_0 is only weakly dependent on I_{max}, increasing from $V_0 = 0.63$ A/m when $I_{max} = 1.5$ T, up to $V_0 = 0.93$ A/m when $I_{max} \lesssim 1$ T.

Materials Not Obeying the Linear Law $\tilde{n} = \tilde{n}_0 + H_{exc}/V_0$

Although the linear law (8) does apply to quite a large number of different cases, we have no *a priori* reason to expect that it should be always valid. Figs. 8–10 report three cases (amorphous Metglas 2605 CO, 50–50 NiFe, GO three-percent SiFe transversally cut) where (8) is actually not obeyed. The $(H_{exc}, \tilde{n})$ representation gives evidence, however, of an interesting feature common to all these cases, the fact that the function $\tilde{n}(H_{exc}; \{P\})$ associated with each material, though nonlinear, is approximately independent of the particular value of I_{max}. Figs. 8(b)–10(b) show in fact that all the loss points of a single material tend to arrange themselves along a single curve, when represented in terms of $\tilde{n}$ versus H_{exc}. This result has immediate interesting practical consequences, since it implies that it is possible to obtain the dependence of dynamic losses on both I_{max} and f_m just from a single curve of P/f_m versus f_m at a fixed value of I_{max}. In fact, this single curve is sufficent to determine the function $\tilde{n}(H_{exc}; \{P\})$, which can then be inserted into (7). By solving this equation with respect to H_{exc}, the dependence of excess losses on $H^{(w)} = 4\sigma G^{(w)} S I_{max} f_m$ (the excess loss will thus

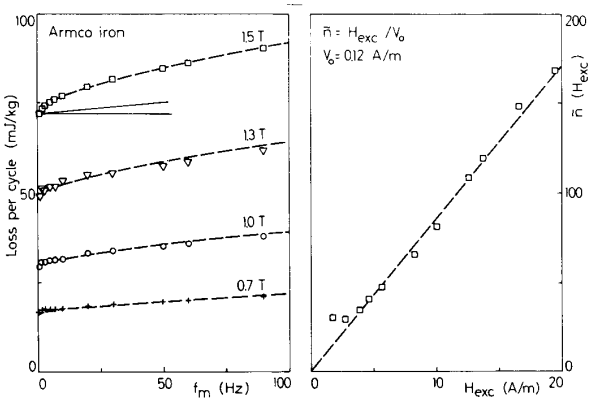

Fig. 5. Power losses in Armco iron. Comment to figure is analogous to that of Figs. 1 and 3. In this material $V_0 = 0.12$ A/m. When $I_{max} < 1.5$ T, dynamic loss is too small with respect to hysteresis loss to permit meaningful use of $(H_{exc}, \tilde{n})$ representation.

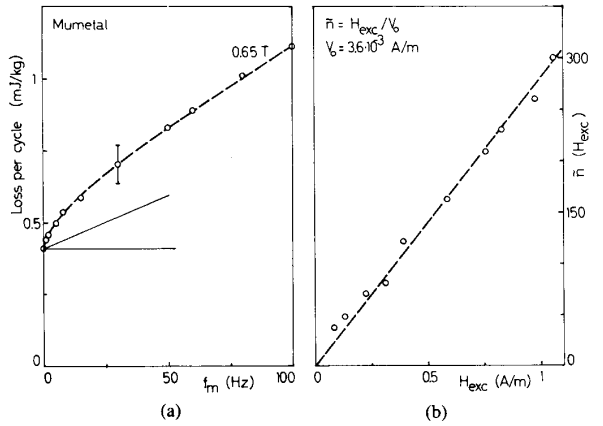

Fig. 6. Power losses in Mumetal. Comment to figure is analogous to that of Figs. 1 and 3. In this material $V_0 = 3.6\ 10^{-3}$ A/m. Due to very low loss figures involved, only measurement at $I_{max} = 0.65$ T was permitted by sensitivity of experimental apparatus.

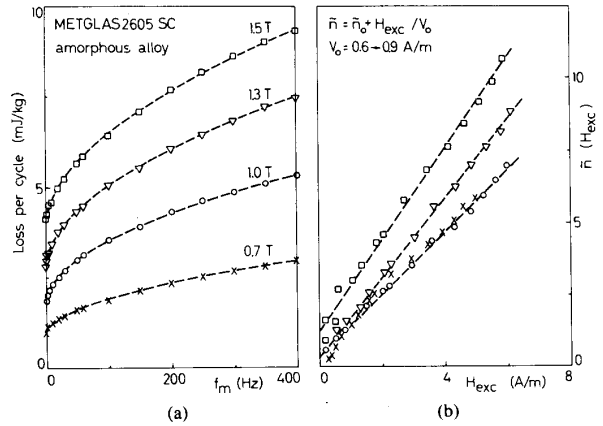

Fig. 7. Power losses in Metglas 2605 SC amorphous alloy. Comment to figure is analogous to that of Fig. 1, but for fact that field V_0 is now no longer strictly constant with respect to I_{max}. We obtain $\tilde{n}_0 = 1.3$, $V_0 = 0.63$ A/m when $I_{max} = 1.5$ T; $\tilde{n}_0 = 0.4$, $V_0 = 0.73$ A/m when $I_{max} = 1.3$ T, $\tilde{n}_0 = 0.4$, $V_0 = 0.93$ A/m when $I_{max} \lesssim 1$ T.

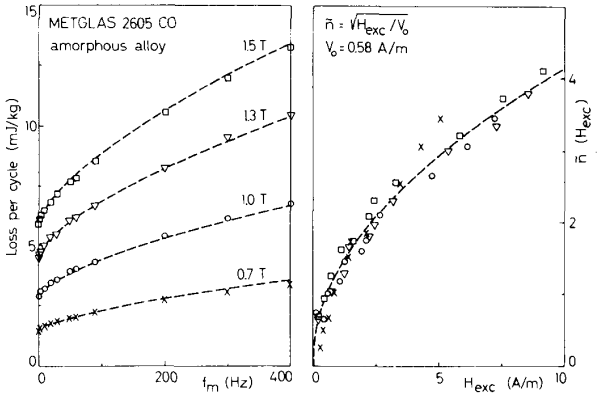

Fig. 8. Power losses in Metglas 2605 CO amorphous alloy. Comment to figure is analogous to that of Fig. 1, but for fact that now experimental points, when represented in terms of $\tilde{n}$ versus H_{exc}, define nonlinear curve which, however, is, to good approximation, independent of I_{max}. This single curve is well described, in this material, by square root law $\tilde{n} = \sqrt{H_{exc}/V_0}$ (broken line of Fig. 8(b)), with $V_0 = 0.58$ A/m.

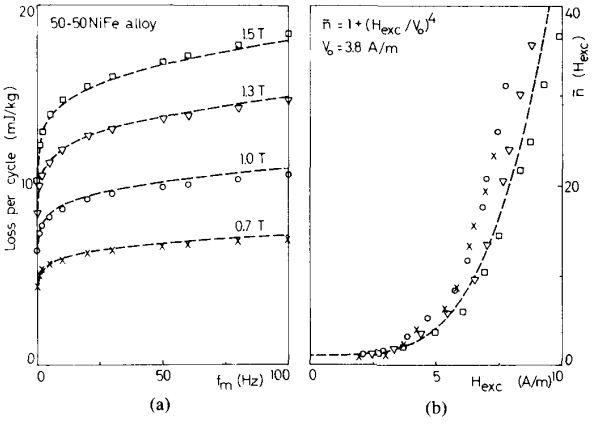

Fig. 9. Power losses in 50-50 NiFe. Comment to figure is analogous to that of Figs. 1 and 8, but $\tilde{n}$ now follow polynomial law $\tilde{n} = 1 + (H_{exc}/V_0)^4$, with $V_0 = 3.8$ A/m.

depend on I_{max} and f_m only through their product $I_{max} f_m$) and on $\{P\}$ is then obtained. This procedure is illustrated by the sets of broken lines shown in Figs. 8(a)–10(a). Each set has been calculated, with the aid of (7), (2), (3), from the corresponding single function $\tilde{n}(H_{exc}; \{P\})$ represented by a broken line in Figs. 8(b)–10(b). It can be seen that, by this procedure, the experimental behavior of dynamic losses is reproduced, in all cases, with an accuracy within a few percent of the total dynamic loss. It is worth remarking that these same conclusions actually apply not only to the three cases here discussed, but also to all the materials, previously considered, which follow the law $\tilde{n} = H_{exc}/V_0$ (see Figs. 3–6).

A proper microscopic interpretation of the behavior of $\tilde{n}(H_{exc}; \{P\})$ in the cases where it is not linear is, at present, still lacking and will be the subject of future investigations.

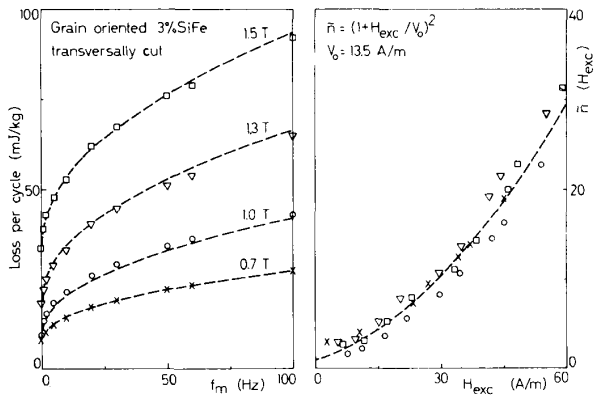

Fig. 10. Power losses in grain oriented three-percent SiFe, cut transversally to rolling direction. Comment to figure is analogous to that of Figs. 1 and 8, but $\tilde{n}$ now follows parabolic law $\tilde{n} = (1 + H_{exc}/V_0)^2$, with $V_0 = 13.5$ A/m.

Hysteresis Losses

Having once discussed the properties of dynamic losses, we briefly look now at the behavior of hysteresis losses versus I_{max}. This can be obtained from the complete sets of loss curves reported in Figs. 1–10 and is represented in Fig. 11, in terms of the hysteresis field $H_{hyst} = P^{(hyst)}/4I_{max}f_m$, which measures the average width of the quasi-static loop. In the figure, we have used full symbols to represent those materials (GO and NO SiFe, Fe, Metglas 2605 SC) for which the linear law (8) of excess losses applies, to draw attention to the fact that these materials are also characterized by a rather similar behavior of H_{hyst}. We believe that this corrspondence is not fortuitous but points at the existence of some direct physical relationship between quasi-static and excess dynamic losses, i.e., between the functions $H_{hyst}(I_{max}; \{P\})$ and $\tilde{n}(H_{exc}; \{P\})$. This possibility was already considered in [20], and the model discussed in Section III for the case of NO SiFe suggests a possible microscopic mechanism whereby this relationship may arise. In this connection, we remark that (15) predicts, with V_0 independent of I_{max}, that H_{hyst} should be proportional to I_{max}. We see from Fig. 11 that, despite the schematic character of that model, this prediction is in fair agreement with experiments. Only when $I_{max} \gtrsim 1.5$ T, a definite deviation takes place.

IV. Dependence of Power Losses on I_{max} and f_m

One of the appealing features of the representation of dynamic losses in the plane (H_{exc}, $\tilde{n}$), discussed in the previous sections, is certainly the fact that it permits one to obtain, with a certain approximation, the complete loss dependence on I_{max} and f_m from a limited amount of input information. Such predicting power of the method—which should be of interest, for instance, in the characterization and optimization of loss figures in electrotechnical steels—will now be illustrated in some detail in a case of clear technological relevance, that of GO three-percent SiFe.

Our information on the loss behavior of this material is

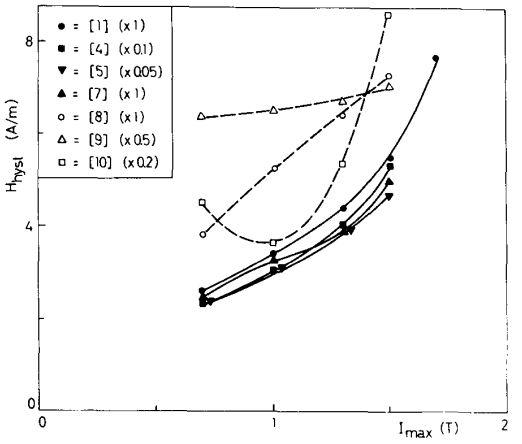

Fig. 11. Behavior versus I_{max} of hysteresis field $H_{hyst} = P^{(hyst)}/4I_{max}f_m$, as obtained from complete sets of loss results reported in Figs. 1-10. Correspondence between various symbols and figure numbers (within square brakets) of Table I is given in inset. Numbers within round brakets represent scale factors by which each set of data has been multiplied.

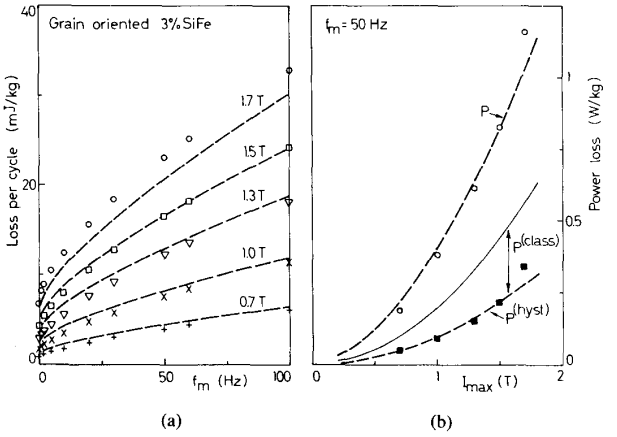

Fig. 12. Grain oriented three-percent SiFe. (a) Same data of Fig. 1(a). (b) Specific illustration of corresponding behavior of total (○) and hysteresis (■) loss per unit mass at f_m = 50 Hz. Broken lines represent predictions of (18), with $C_0 = 1.92 \times 10^{-3}$ J · kg^{-1} T^{-2}, $C_1 = 5.9 \times 10^{-4}$ J · s$^{1/2}$ kg^{-1} T$^{-3/2}$.

summarized by Fig. 12, where the same loss data of Fig. 1(a) are again reported, together with a specific illustration of the dependence on I_{max} of total and hysteresis losses P and $P^{(hyst)}$ at f_m = 50 Hz. To interpret these data, let us consider what we have learnt in the previous sections about the behavior of the terms which, according to the separation of losses (3), contribute to the total loss P. As to the hysteresis loss $P^{(hyst)}$, we have seen (Fig. 11) that the hysteresis field $H_{hyst} = P^{(hyst)}/4I_{max}f_m$ is, in this material, approximately proportional to I_{max}, so that $P^{(hyst)} \propto I_{max}^2 f_m$ (a similar result is reported in [25]). This should be a good approximation at least in the range $I_{max} \lesssim 1.5$ T. The excess loss $P^{(exc)}$, on the other hand, is described in general by (9). However, if we limit ourselves to sufficiently high magnetizing frequencies (say $f_m \gtrsim 20$ Hz), we can use the approximate simplified expression (10) and further neglect the small term $\tilde{n}_0 V_0/4$. With these approximations, and taking into account that the field V_0 in (10) is independent of I_{max}, we can therefore express the total loss per unit mass as

$$P/\delta \simeq C_0 I_{max}^2 f_m + \frac{\pi^2 \sigma d^2}{6\delta} (I_{max} f_m)^2 + C_1 (I_{max} f_m)^{3/2} \quad (18)$$

where (2) has been used to express the classical loss and C_0, C_1 are suitable constants characterizing the material. Since C_0 and C_1 are the only unknown parameters of (18), the knowledge of two experimental points is sufficient to determine their values and consequently to predict the complete dependence of P/δ on both I_{max} and f_m. In the case of the data of Fig. 12, we have determined the values of C_0 and C_1 from two points, $f_m = 0$ and f_m = 50 Hz, of the loss curve measured at I_{max} = 1.5 T. We have then made use of (18) to predict the loss behavior in the whole investigated range of I_{max} and f_m values. The result is represented by the set of broken lines in Fig. 12. We can see that the agreement between (18) and the whole set of experimental points is within ±10 percent when $f_m \gtrsim 20$ Hz. The deviations at high peak magnetizations ($I_{max} >$ 1.5 T) are due to the fact that the expression we have used for the hysteresis loss becomes a bad approximation, while those at low I_{max} arise from neglecting the term $\tilde{n}_0 V_0/4$ of (10). Actually, this term becomes more and more important with decreasing I_{max}, since $\tilde{n}_0$ progressively increases, while, at the same time, the first term of (10) decreases as $\sqrt{I_{max}}$. Incidentally, these considerations show that both these sources of error should be small around 1.5 T, so that the values of C_0 and C_1 are indeed best determined by considering, as we have done, the loss curve corresponding to I_{max} = 1.5 T. Of course, (18) could be applied not only to GO SiFe, but in general to any material obeying the linear law (8) or (12), with V_0 independent of I_{max} and H_{hyst} approximately proportional to I_{max} (see Figs. 3-6 and 11).

Equation (18) gives evidence of the existence of two basic contributions to the dependence of the total loss P/δ on I_{max} at a fixed magnetizing frequency, one proportional to I_{max}^2, the other to $I_{max}^{1.5}$. The average exponent expressing the law of dependence of P/δ on I_{max} is therefore expected to be included between 1.5 and 2, depending on the values of C_0 and C_1 in (18). This conclusion should be compared with old empirical rules, often mentioned in the literature [5], expressing P as $P \sim I_{max}^{1.7}$. Our treatment provides a physical interpretation to these rules and shows how they may arise from the interplay of the three terms which, according to (3), contribute to power losses.

V. Conclusion

The theoretical interpretation of the experimental results on power losses in soft materials presented in this paper has shown that the function $\tilde{n}(H_{exc}; \{P\})$ defined in Section II provides a promising convenient tool to look into the connection between dynamic losses and micro-

structure of soft materials. In several cases, a single function $\tilde{n}(H_{exc}; \{P\})$ can be associated with a given material, even when loss curves at different peak magnetizations are considered and when—as in GO SiFe—a dependence of $\tilde{n}$ on I_{max} is observed, it provides additional information on the magnetic domain structure. These results suggest focusing theoretical efforts on the study of the properties of $\tilde{n}$ in different physical situations. Adopting this point of view has permitted us to give a natural interpretation of the general presence of nonlinearities in the behavior of the loss per cycle of any material, and to achieve a quantitative prediction of excess losses in fine grained laminations (see (12)–(17)). However, even in the cases where we are not yet able to predict the properties of $\tilde{n}$ from a microscopic model, the very fact that a single function $\tilde{n}(H_{exc}; \{P\})$ can be associated with a given material has relevant practical consequences. In fact, $\tilde{n}$ can then be obtained from a single loss curve measured at a given value of I_{max}, and, through (7), the complete dependence of dynamic losses on both I_{max} and f_m can then be worked out. By making use of this result and of some additional information on the dependence of hysteresis losses on I_{max}, we have shown in Section IV that, in GO SiFe, it is possible to predict the behavior of the total loss on I_{max} and f_m from the knowledge of only two points of a single loss curve, with an approximation that, for the data presented in this paper and in the range $f_m \geq 20$ Hz, is within ± 10 percent. Developing general microstructural models of the behavior of $\tilde{n}(H_{exc}; \{P\})$ in various materials appears now as the main objective of future investigations.

Acknowledgment

The author is deeply indebted to Prof. G. Montalenti, Prof. A. Ferro Milone, and Dr. F. Fiorillo for their constant encouragement and interest in this work, a number of fruitful discussions, and valuable comments and suggestions after their critical reading of the manuscript. He also wishes to thank E. Genova, A. Gobetto, S. Rocco, and C. Visca for their technical assistance in loss measurements.

References

[1] J. W. Shilling and G. L. Houze, Jr., "Magnetic properties and domain structure in grain-oriented 3% Si-Fe," *IEEE Trans. Magn.*, vol. MAG-10, pp. 195–223, 1974.
[2] C. D. Graham, Jr., "Physical origin of losses in conducting ferromagnetic materials," *J. Appl. Phys.*, vol. 53, pp. 8276–8280, 1982.
[3] G. Bertotti, "Space-time correlation properties of the magnetization process and eddy current losses: Theory," *J. Appl. Phys.*, vol. 54, pp. 5293–5305, 1983.
[4] ——, "A general statistical approach to the problem of eddy current losses," *J. Magn. Magn. Mater.*, vol. 41, pp. 253–260, 1984.
[5] R. M. Bozorth, *Ferromagnetism*. New York: Van Nostrand, 1951, ch. 17.
[6] R. H. Pry and C. P. Bean, "Calculation of the energy loss in magnetic sheet materials using a domain model," *J. Appl. Phys.*, vol. 29, pp. 532–533, 1958.
[7] A. Ferro, G. Montalenti, and G. P. Soardo, "Non linearity anomaly of power losses vs. frequency in various soft magnetic materials," *IEEE Trans. Magn.*, vol. MAG-11, pp. 1341–1343, 1975.
[8] K. Matsumura and B. Fukuda, "Recent developments of non-oriented electrical steel sheets," *IEEE Trans. Magn.*, vol. MAG-20, pp. 1533–1538, 1984.
[9] G. Bertotti, G. Di Schino, A. Ferro, and F. Fiorillo, "On the effect of grain size on magnetic losses of 3% non-oriented SiFe," *J. de Physique*, vol. 46-C6, pp. 385–388, 1985.
[10] J. W. Shilling, "Domain structures in 3% Si-Fe single crystals with orientation near (110) [001]," *IEEE Trans. Magn.*, vol. MAG-9, pp. 351–356, 1973.
[11] G. Bertotti, F. Fiorillo, and M. P. Sassi, "A new approach to the study of loss anomaly in SiFe," *IEEE Trans. Magn.*, vol. MAG-17, pp. 2852–2856, 1981.
[12] K. Narita and M. Imamura, "Frequency dependence of iron losses in 4-percent Si-Fe single crystal with (100) [001] orientation," *IEEE Trans. Magn.*, vol. MAG-15, pp. 981–988, 1979.
[13] M. Celasco, A. Masoero, P. Mazzetti, and A. Stepanescu, "Study of Bloch wall dynamics and losses in monocrystalline, polycrystalline, and amorphous materials by means of optical techniques," *J. Appl. Phys.*, vol. 57, pp. 4238–4243, 1985.
[14] Y. Sakaki, "An approach estimating the number of domain walls and eddy current losses in grain-oriented 3% Si-Fe tape wound cores," *IEEE Trans. Magn.*, vol. MAG-16, pp. 569–572, 1980.
[15] Y. Sakaki and S.-I. Imagi, "Relationship among eddy current loss, frequency, maximum flux density and a new parameter concerning the number of domain walls in polycrystalline and amorphous soft magnetic materials," *IEEE Trans. Magn.*, vol. MAG-17, pp. 1478–1480, 1981.
[16] J. E. L. Bishop, "Eddy current dominated magnetization processes in grain oriented silicon iron," *IEEE Trans. Magn.*, vol. MAG-20, pp. 1527–1532, 1984.
[17] P. Mazzetti, "Bloch walls correlation and magnetic loss in ferromagnets," *IEEE Trans. Magn.*, vol. MAG-14, pp. 758–763, 1978.
[18] J. E. L. Bishop, "Enhanced eddy current loss due to domain displacement," *J. Magn. Magn. Mater.*, vol. 49, pp. 241–249, 1985.
[19] G. Bertotti, "Space-time correlation properties of the magnetization process and eddy current losses: Applications," *J. Appl. Phys.*, vol. 55, pp. 4339–4355, 1984.
[20] ——, "Physical interpretation of eddy current losses in ferromagnetic materials," *J. Appl. Phys.*, vol. 57, pp. 2110–2126, 1985.
[21] ——, "Some considerations on the physical interpretation of eddy current losses in ferromagnetic materials," *J. Magn. Magn. Mater.*, vols. 54–57, pp. 1556–1560, 1986.
[22] ——, "Direct relation between hysteresis and dynamic losses in soft magnetic materials," *J. de Physique*, vol. 46-C6, pp. 389–392, 1985.
[23] H. J. Williams, W. Shockley, and C. Kittel, "Studies of the propagation velocity of a ferromagnetic domain boundary," *Phys. Rev.*, vol. 80, pp. 1090–1094, 1950.
[24] B. D. Cullity, *Introduction to Magnetic Materials*. Reading, MA: Addison-Wesley, 1972, ch. 13.
[25] J. G. Benford, "Separation of losses in oriented silicon steels from 0.13 to 0.34 mm thick," *IEEE Trans. Magn.*, vol. MAG-20, pp. 1545–1547, 1984.

Giorgio Bertotti was born in Vercelli, Italy, in 1952. He received the physics degree from the University of Torino, Italy, in 1976.

After a period of two years spent at FIAT Research Center, Torino, he has been with the Istituto Elettrotecnico Nazionale Galileo Ferraris since 1979. His main field of interest is the investigation of hysteresis phenomena and magnetization processes in soft magnetic materials.